# The Adaptive Content and Contrast-aware Technique for Visible Watermarking*

Min-Jen Tsai and Jung Liu
Institute of Information Management
National Chiao Tung University, R.O.C.
mjtsai@cc.nctu.edu.tw
rongrong211@gmail.com

Ching-Hua Chuang
Department of Information Management, Tahwa
Institute of Technology, R.O.C.
chuang@thit.edu.tw

***Abstract*—The efficiency of a digital image watermarking technique depends on the preservation of visually significant information. This is attained by embedding the watermark transparently with the maximum possible strength. This paper presents an Adaptive approach for still image in which the watermark embedding process employs the wavelet transform and incorporates Human Visual System (HVS) characteristics. The sensitivity of a human observer to contrast with respect to spatial frequency is described by the Contrast Sensitivity Function (CSF). The strength of the watermark within the decomposition sub-bands is adjusted according to this sensitivity. Moreover, the watermark embedding process is carried over the sub-band coefficients by the analysis of Noise Visibility Function (NVF) in which the distortions are less noticeable. Such unique design is novel and the experimental evaluation of the proposed method shows excellent results in terms of robustness and transparency.**

***Keywords- Image Watermarking; HVS; CSF; wavelet.***

## I. INTRODUCTION

Due to the advancement of digital technologies and rapid communication network deployment, digital images are now widely distributed on the Internet or via other digital devices. Digital image allows an unlimited number of copies from an "original", people can acquire or distribute the images without any reduction in quality through both authorized and unauthorized distribution channels. With the ease of editing and reproduction, protection of the intellectual property right and authentication of digital multimedia becomes an important issue.

In recent years, digital watermarking has been extensively studied and regarded as a potentially effective means for protecting copyright ownership of digital media content [1], since it makes possible the embedding of secret information in the digital content to identify the copyright owner. Many researchers have invented various visible watermarking schemes to protect copyrights. From the literature survey, Chen [2] proposed a visible watermarking mechanism to embed a watermark by a statistic approach. They divided the image into equal-sized blocks and calculated the standard deviation of those pixels in block. They later calculated the embedding ratio of watermark into the corresponding pixels for watermarking. Chen et al. [3] describe an approach for adaptive visible watermarking based on the analysis of the threshold value of the image using Otsu's threshold to select the best embedding strength of the watermark at a particular position. Huang and Tang [4] presented a contrast sensitive visible watermarking scheme with the assistance of human visual system (HVS). They computed the contrast sensitive function (CSF) mask from discrete wavelet transform domain and used a square function to determine the mask weights for each sub-band. At last, they adjusted the embedding weights based on the block classification with the texture sensitivity of HVS. Tsai [5] incorporated the collaboration of CSF and noise visible function (NVF) for HVS models and proposed a new visible watermarking technique where the intensity of the watermark in different regions of the image depends on the underlying content of the image and humans' sensitivity to spatial frequencies. However, the previous works extended the following issues:

1. Since the applications of visible watermarking are often limited to content browsing or previewing, content viewers are annoyed at degraded visual quality. Therefore, the embedded patterns should be unobtrusive. However, the robustness of watermarking and quality of the digital content are generally conflicted with each other.
2. The embedding factors for watermarking emphasize different weights in various frequency domains. Subsequently, certain thresholds should be examined carefully during the design of watermarking schemes.

The goal of this paper is to present an adaptive visible watermarking algorithm (ACOCOA) with a novel contrast sensitivity function masking for wavelet based watermarking method which considers the characteristics in different frequency domain. The main contribution of this paper is to leverage the knowledge of Contrast Sensitivity Function and Noise Visibility Function to embed low energy in the area where the sensitivity of CSF is high and vice versa. The experimental results demonstrate that the proposed technique improves the watermarked image quality, translucence and robustness of the watermarking.

The rest of this paper is organized as follows. In Section 2, we will give the detailed description of the proposed theoretical approach for watermarking technical. In Section 3, numerical results and discussion are illustrated to justify the proposed approach. Finally, the conclusion is drawn in Section 4.

 ISBN: 978-1-61208-166-3 

## II. THE ACOCOA WATERMARKING ALGORITHM

The most important requirements in the visible watermarking scheme are the robustness and translucence, but unfortunately they are in confliction with each other. If we increase the energy of watermark to improve its robustness, the problem we get is perceptual translucence decreasing with less image fidelity and vice versa. We find the critical factor "HVS" in providing the good translucence of the watermarked image and a better robustness [4]. HVS research offers the mathematical models about how humans see the world. Hemanmi [6] applied uniform quantization noise to measure the psychovisual sensitivity in wavelet sub-bands within an image and showed the results that human vision has different sensitivity from various spatial frequencies (frequency sub-bands). The HVS by using the contrast sensitive function (CSF) and noise visibility function (NVF) is integrated in this study and will be explained in brief as following:

### A. *CSF (Contrast Sensitive Function)*

Mannos and Sakrison [7] originally presented a model of the CSF for luminance (or grayscale) images is given as follows:

$$H(f) = 2.6 \times (0.0192 + 0.114 \times f) \times e^{-(0.114 \times f)^{1.1}} \qquad (1)$$

where $f = \sqrt{f_x^2 + f_y^2}$ is the spatial frequency in cycles/degree of visual angle ($f_x$ and $f_y$ are the spatial frequencies in the horizontal and vertical directions, respectively). The HVS is most sensitive to normalized spatial frequencies between 0.025 and 0.125 and less sensitive to low and high frequencies.

CSF masking [8], [9] is one way to apply the CSF in the discrete wavelet domain. CSF masking refers to the method of weighting the wavelet coefficients relative to their perceptual importance. In [9], the DWT CSF mask utilizes the information in all of the approximation sub-bands as well as all of the detail sub-bands to yield 11 unique weights in the mask. All of the weights are normalized so that the lowest weight is equal to one. The 11 weights of DWT CSF mask are shown in Figure 1 after 5-level wavelet pyramidal DWT decomposition and the HVS is most sensitive to the distortion in mid-frequency regions (level 3) and sensitivity falls off as the frequency value drifts on both sides (level 1, 2, 4 and 5). The square function in [4] is applied to approximate the effect of CSF masking. The adequate modulation rate $\beta^{\lambda}$ for each sub-band is determined by:

$$\beta^{\lambda} = 0.01 + \frac{(7.20 - r^{\lambda})^2}{7.20^2} \qquad (2)$$

where $r^{\lambda}$ represents the wavelet coefficient CSF of the perceptual importance weight for each sub-band where λ denotes the decomposition level.

### B. *NVF (Noise Visibility Function)*

Alexander et al. [10] presented a stochastic approach based on the computation of a NVF (Noise Visibility Function) that characterizes the local image properties and identifies texture and edge regions. This allows us to determine the optimal watermark locations and strength for the watermark embedding stage. The adaptive scheme based on NVF calculated from stationary GG model is superior to other schemes, which is defined as follows:

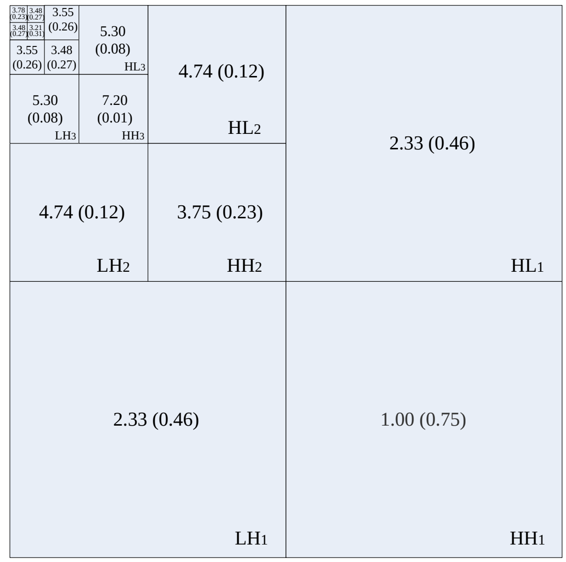


Figure 1. A five-level wavelet pyramidal decomposition. $r^{\lambda}(\beta_{\lambda,\theta})$ values for each level λ are indicated at the center of each band.

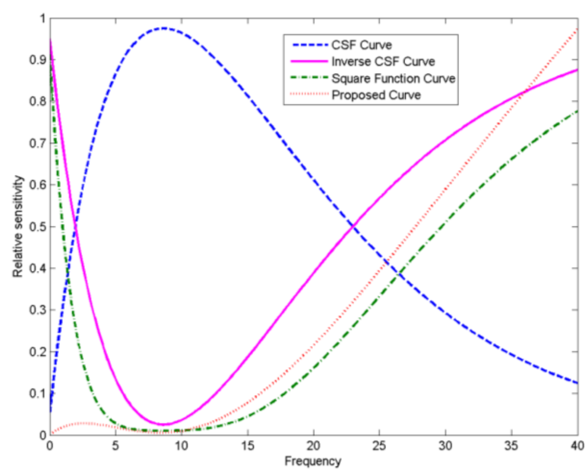


Figure 2. The sensitivity curve of CSF, inverse CSF, square function and proposed cruve.

TABLE I. ADAPTIVE CSF MASKING FOR A FIVE-LEVEL DWT

| Orien-tation | Level | | | | |
|---|---|---|---|---|---|
| | 1 | 2 | 3 | 4 | 5 |
| LL | | | | | 0.000001 |
| HL/ LH | 0.599316 | 0.211279 | 0.031660 | 0.032198 | 0.031905 |
| HH | 1.000000 | 0.341371 | 0.005418 | 0.031905 | 0.030574 |

 ISBN: 978-1-61208-166-3

$$NVF_{x,y} = \frac{w_{x,y}}{w_{x,y} + \sigma_I^2} \qquad (3)$$

where $w_{x,y} = \gamma[\eta(\gamma)]^{\gamma} / \left\| r_{x,y} \right\|^{2-\gamma}$ and $\sigma_I^2$ is the global variance of the original image. $\eta(\gamma) = \sqrt{\Gamma(3/\gamma)/\Gamma(1/\gamma)}$, $\Gamma(s) = \int_0^{\infty} e^{-u} u^{s-1} du$ (gamma function) and $r_{x,y} = \frac{I_{x,y} - \bar{I}_{x,y}}{\sigma_I}$, $\gamma$ is the shape parameter and $r_{x,y}$ is determined by the local mean and the local variance. For most of real images, the shape parameter is in the range $0.3 \le \gamma \le 1$. In our scheme, the estimated shape parameter for $\gamma = 0.65$, and width of window is 1.

### *C. Adaptive CSF masking*

The property of CSF is a measure of fundamental spatiochromatic of the HVS, and people are more sensitive in mid-frequency regions. Therefore, we need embed low intensity of visible watermarking in high sensitivity regions and vice versa. According to such observation, we can draw the inverse CSF as shown in Figure 2, which represents the embedding intensity allowed based on the study of HVS. Therefore, a good visible watermarking should embed low energy in mid-frequency regions from the plot of inverse CSF to avoid obtrusiveness and affect the visual quality. Consequently, the square function applied in [4-5] dose not match the perfect inverse CSF curve as shown in Figure 2 so they need to set certain thresholds to avoid adding too much energy in the low DWT frequency domains. In order to solve the problems and obtain the better watermarked image for HVS that contains the characteristics of robustness and translucence, we use the interpolation method to construct the Adaptive CSF masking to improve the HVS model for better image quality. From above discussion, we have proposed an Adaptive CSF masking, which is defined in formula (4) and tabulated the corresponding coefficients of the associated sub-bands in Table 1:

$$\text{Adaptive CSF masking} = (1 - H(f)) \times f \qquad (4)$$

Since LL band is very critical during the reconstruction of the image, a small value of parameter is derived in order to preserve the quality of watermarked image. According to such observation, we also draw the proposed curve as shown in Figure 2, which can help us to compare the different watermark weighting curve.

### *D. ACOCOA Visible Watermarking Algorithm*

ACOCOA algorithm leverages the study of [5] and modifies the controlling parameters of watermark embedding based on the consideration of the image quality. The watermark embedding procedures are briefly described as following steps and the flow chart is shown in Figure 3:

Step 1. The original color image is converted in the color space domain from RGB to YCrCb.

Step 2. By using Bi9/7 filter from [11], compute the 5-level 2-D wavelet coefficients of Y component from original color image and grayscale logo watermark image.

Step 3. Modify the DWT coefficients of the host image by

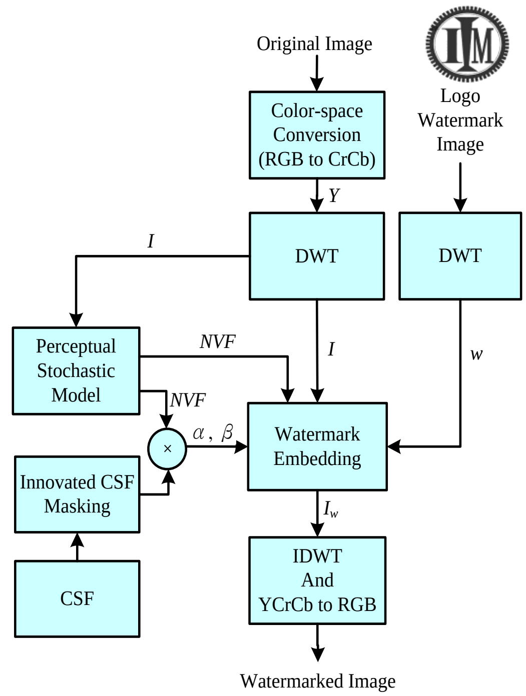


Figure 3. The flow chart of ACOCOA visible watermarking.

TABLE II. PSNR (DB) SUMMARY OF WATERMARKED COLOR IMAGES

| Method / Image | Method of [4] | Method of [5] | I-COCOA |
|---|---|---|---|
| Lena | 26.78 | 32.67 | 36.21 |
| Lake | 26.03 | 31.66 | 33.95 |
| Peppers | 26.83 | 32.48 | 35.29 |
| F16 | 27.96 | 32.43 | 34.87 |
| Tiffany | 27.57 | 32.92 | 34.64 |
| Splash | 25.68 | 32.37 | 36.78 |

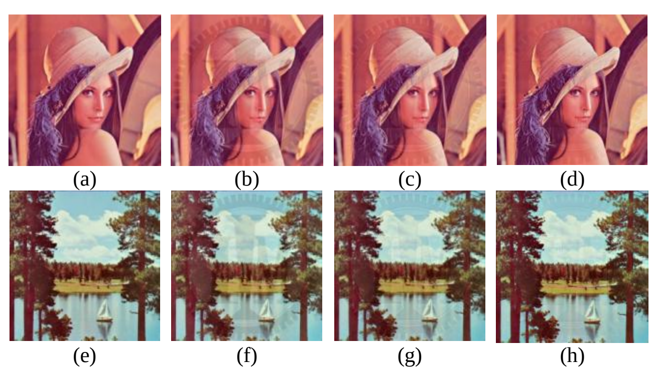


Figure 4. The visual quality comparison of original and watermarked images. (a), (e) are original Lena, Lake images respectively. (b), (f) are watermarked images by the method of [4]. (c), (g) are watermarked images by the method of [5]. (d), (h) are watermarked images by the ACOCOA method.

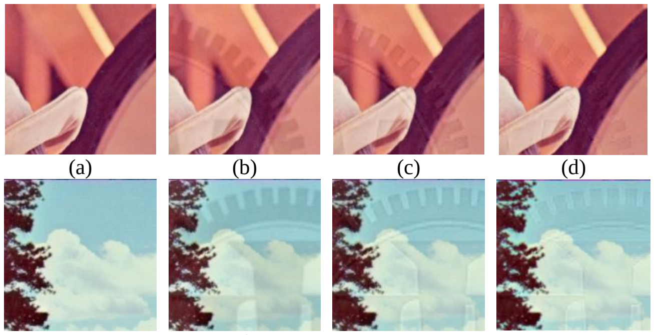

(a) (b) (c) (d)

(e) (f) (g) (h)

Figure 5. The visual quality comparison of close-ups for images in Figure 4 (a),(e) are original Lena, Lake images. (b),(f) are watermarked images by the method of [4]. (c),(g) are watermarked images by the method of [5]. (d),(h) are watermarked images by the ACOCOA method.

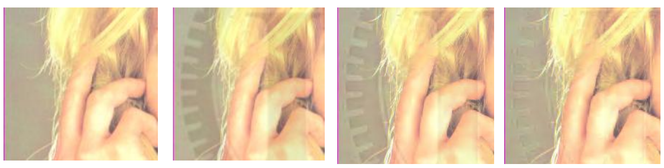

(a) (b) (c) (d)

Figure 6. The visual quality comparison of close-ups for Tiffany image after JPEG 2000 compression. (a) original image, (b) watermarked image by the method of [4], (c) watermarked image by the method of [5], (d) watermarked images by the ACOCOA method.

TABLE III. PSNR (DB) SUMMARY OF WATERMARKED COLOR IMAGES BEFORE AND AFTER JPEG 2000 COMPRESSION.

| Method / Image | Method of [4] | | | Method of [5] | | | I-COCOA Approach | | |
|---|---|---|---|---|---|---|---|---|---|
| | (1) | (2) | (3) | (1) | (2) | (3) | (1) | (2) | (3) |
| Lena | 26.78 | 24.40 | 28.41 | 32.67 | 27.06 | 28.52 | 36.21 | 27.92 | 28.69 |
| Lake | 26.03 | 23.02 | 26.30 | 31.66 | 25.06 | 26.61 | 33.95 | 25.72 | 27.04 |
| Peppers | 26.83 | 24.44 | 28.42 | 32.48 | 27.03 | 28.50 | 35.29 | 27.83 | 28.75 |
| F16 | 27.96 | 24.94 | 28.00 | 32.43 | 26.71 | 28.13 | 34.87 | 27.37 | 28.38 |
| Tiffany | 27.57 | 25.09 | 28.60 | 32.92 | 27.36 | 28.71 | 34.64 | 27.86 | 28.93 |
| Splash | 25.68 | 24.01 | 29.30 | 32.37 | 27.53 | 29.31 | 36.78 | 28.70 | 29.34 |

Note:
(1) means the PSNR values before the JPEG 2000 compression.
(2) means the PSNR values after the JPEG 2000 compression.
(3) means the PSNR values are compared between the compressed watermarked image and the watermarked image.

using the following equation:

$$I^{w}_{x,y} = \alpha_{\lambda,\theta} \times I_{x,y} + (\beta_{\lambda,\theta} + NVF_{x,y}) \times w_{x,y} \qquad (5)$$

Note: $(x,y)$ indicates the spatial location. $I$ and $w$ are the decomposed wavelet coefficients of the original image and the logo watermark image. $\alpha_{\lambda,\theta}$ and $\beta_{\lambda,\theta}$ are scaling and embedding factors which are defined as below. $NVF_{x,y}$ is defined in formula (3).

$$\beta_{\lambda,\theta} = (1 - NVF_{x,y}) \times (1 - H(f)) \times f \qquad (6)$$

$$\alpha_{\lambda,\theta} = 1 - 0.7\beta_{\lambda,\theta} \qquad (7)$$

Step 4. Inverse transform the DWT coefficients of the original image to obtain the watermarked image.

## III. EXPERIMENTAL RESULTS

The proposed visible watermarking algorithm has been implemented and intensively tested by using the widely available color images from USC image database [12] and the performance of 512×512 experimental images are tabulated in Table 2 for comparison purpose. The grayscale watermark of logo image adopted in the experiments is a department logo and shown in Figure 3.

In order to make a fair comparison with the method from [4], [5], it is better to embed the same watermark for the same cover image. However the watermark used in [4] is not available currently, we embed the logo watermark from Figure 3 to make the best effort for performance comparison. The performance analysis can be categorized as follows:

### A. *PSNR (peak signal-to-noise ratios)*

The tabulated results from Table 2 disclose that our watermarking scheme can achieve higher PSNR values than the method in [4] and [5] where the PSNRs are generally below 33dB for different images. The low PSNRs have positive correlation with the degradation in image quality. This denotes the fidelity of images from our method is better than the traditions CSF based method.

### B. *Visual Quality*

Figure 4 (a) and 4(e) illustrate the original cover images of Lena and Lake from [12], the results of watermarked images from [4] and [5] are compared with the proposed approach and the results are in Figure 4 (b)(c)(d) and (f)(g)(h).

From Figure 4 (b)(c)(d) and (f)(g)(h) image pairs, the proposed method has the closest luminance maintenance compared with the original ones which are shown clearly and unobtrusive from the photos. The watermarked images by using [4] and [5] have more bright effect in the unmarked areas. To further compare the details from the watermarked images, Figure 5 (a)(e) are the close-ups of original images. Figure 5 (b)(f) are the close-ups of Figure 4 (b)(f) by using [4]'s method. Figure 5 (c)(g) are the close-ups of Figure 4 (c)(g) by using [5]'s method. Figure 5 (d)(h) are the close-ups of Figure 4 (d)(h) by using our proposed method. It is very clear that the watermark's edges and thin lines are blurred and obtrusive in those images by using the method of [4] and [5] but the watermark patterns in our method still has sharp edge and the logo watermark is evidently embedded.

### C. *JPEG 2000 Compression*

The robustness of the proposed visible watermark technique should be tested for compression attack. For JPEG

 ISBN: 978-1-61208-166-3 

2000 compression, software from [13] is adopted as the compression tool. Figure 6 (d) is the close-up of watermarked image after JPEG 2000 compression by the proposed method. It is apparent that the logo pattern is still evidently existed and recognized. The PSNR values before and after the JPEG 2000 compression are tabulated in Table 3. The compression ratio is 100:3 between the uncompressed image and compressed image.

Other attacks from [14] are also preformed and the experimental results are consistent with the above findings which indicate our visible watermarking scheme has better visual effect and high PSNR values than other schemes like [4] and [5]. In summary, an intensive comparison for proposed ACOCOA technique has been illustrated above. Therefore, we can conclude that the proposed method is more robust with better image quality than the algorithm in [4] and [5].

## IV. CONCLUSION AND FUTURE WORKS

In this study, we have proposed a novel watermarking technique I-COCOA where the intensity of the watermark in different regions of the image depends on the underlying content of the image and HVS to spatial frequencies for copyright protection. The Adaptive CSF masking is fine tuned for watermark embedding which results significant improvement in terms of the image quality, translucence and robustness of the watermarking. The experimental results demonstrate the proposed ACOCOA visible watermarking scheme has achieved high PSNR values with better visual fidelity and robustness to attacks than other schemes.

## ACKNOWLEDGMENT

This work was partially supported by the National Science Council in Taiwan, Republic of China, under Grant NSC99-2410-H-009-053-MY2.

## REFERENCES

[1] I.J. Cox, J. Kilian, F.T. Leighton, and T. Shamoon, "Secure spread spectrum watermarking for multimedia," *IEEE Transactions On Image Processing*, vol. 6, no. 12, pp. 1673–1687, Dec. 1997.

[2] P.M. Chen, "A visible watermarking mechanism using a statistic approach," *5th International Conference on Signal Processing Proceedings*, vol. 2, pp. 910–913, 2000.

[3] J.J. Chen, T.M. Ng, A. Lakshminarayanan and H.K.Garg, "Adaptive visible watermarking using Otsu's Thresholding," International Conference on Computational Intelligence and Software Engineering, pp. 1–4, Dec. 2009.

[4] B.B. Huang and S.X. Tang, "A contrast-sensitive visible watermarking scheme," *IEEE Multimedia*, vol. 13, no.2, pp. 60–66, Apr.-Jun. 2006.

[5] M.J. Tsai, "A Visible Watermarking Algorithm Based on the Content and Contrast Aware (COCOA) Technique," *Journal of Visual Communication and Image Representation*, vol. 20, issue 5, pp. 323–338, July 2009.

[6] S.S. Hemami, "Visual Sensitivity Considerations for Subband Coding," Proceedings of Thirty-first Asilomar Conference on Signals, Systems, and Computers, Pacific Grove, CA, vol. 1, pp. 652-656, Nov. 1997.

[7] J.L. Mannos and D.J. Sakrison, "The effects of a visual fidelity criterion on the encoding of image," *IEEE Transactions on Information Theory*, vol. 20, no. 4, pp. 525–536, July 1974.

[8] D. Levický and P. Foriˇs, "Human Visual System Models in Digital Image Watermarking," *RADIOENGINEERING*, vol.13, no. 4, pp. 38–43, Dec. 2004.

[9] A.P. Beegan, L.R. Iyer, and A.E. Bell, "Design and Evaluation of Perceptual Masks for Wavelet Image Compression," *IEEE Digital Signal Processing Workshop*, IEEE CS Press, pp. 88–93, Oct. 2002.

[10] S. V. Alexander, Z. A. Herrigel and N. Baumgaertner, "A stochastic approach to content adaptive digital image watermarking," *in Proc. 3rd Int. Workshop Information Hiding*, Dresden, Germany, pp. 211–236, Sep. 1999.

[11] A.B. Watson, G.Y. Yang, J.A. Solomon and J. Villasenor, "Visibility of wavelet quantization noise," *IEEE Transactions On Image Processing*, vol. 6, no. 8, pp. 1164–1175, Aug. 1997.

[12] USC SIPI – The USC-SIPI Image Database., Retrieved Aug. 18, 2011, from http://sipi.usc.edu/database/

[13] JPEG 2000 compression, Retrieved Aug. 18, 2011, from http://www.ece.uvic.ca/ ~mdadams/jasper/

[14] StirMark, Retrieved Aug. 18, 2011, from http://www.petitcolas.net/fabien/ software/StirMarkBenchmark_4_0_129.zip